CERN/EF/RF 86-1
4 March 1986

# ON NIOBIUM COATED COPPER CAVITIES AT 500 MHz

G. Arnolds-Mayer[2], C. Benvenuti[1], D. Bloess[1], G. Cavallari[1], E. Chiaveri[1], M. Hauer[1], N. Hilleret[1], M. Minestrini[4], V. Palmieri[5], L. Ponto[3], F. Scalambrin[1] and W. Weingarten[1]

1 CERN, European Organization for Nuclear Research, Geneva, Switzerland
2 Sc. Ass. from University of Wuppertal, FRG
3 Sc. Ass. from Politechnika Warszawska, Poland
4 Technical Student from University of Perugia, Italy
5 Technical Student from University of Naples, Italy

## ABSTRACT

To upgrade LEP from the initially 50 GeV to higher energies superconducting accelerating structures have to be installed. Accelerating fields of at least 5 MV/m are required, which now are reached reliably with cavities made from very pure niobium sheet or from niobium coated copper cavities. This paper reports about niobium coated 500 MHz cavities made from oxygen free high conductivity (OFHC) copper. The niobium films are deposited by a bias diode or by a magnetron sputtering configuration. At 4.2 K and at low fields quality factors ranged up to $4.2 * 10^9$. At the present design field of the LEP-machine of 5 MV/m Q lies between $1.5 * 10^9$ and $1.9 \pm 10^9$. The maximum accelerating field so far achieved is 10.8 MV/m, while 8 MV/m are obtained reproducibly.

3203G/GAM/ed

## 1. INTRODUCTION

To enhance the thermal stability of superconducting accelerator structures which can be used to upgrade LEP above 50 GeV two lines are followed at CERN: the use of high purity niobium for cavities formed from niobium sheet material [1] and the sputter coating of niobium films on cavities made from OFHC copper [2]. High purity niobium as well as copper have thermal conductivities considerably larger than the one of the niobium usually used until the early 80th, leading to higher quench fields [3]. Provided that the niobium/copper composite can be produced by a simple industrial process the cavity cost can be reduced considerably as the material price which is now about 20% would be negligible.

## 2. PREPARATION OF THE NIOBIUM COATED COPPER CAVITIES

In this chapter a short survey of the production steps of the niobium coated copper cavities will be given. The fabrication procedures are described in detail elsewhere [4].

### 2.1 Preparation of the copper cavities

The 500 MHz single cell cavities are fabricated from 3 mm OFHC copper sheet material. The half cells are formed by spinning on a lathe, the cutoff tubes are rolled. Tubes and half cells are generally electron beam welded. The vacuum flanges are electron beam welded or brazed to the cutoff tubes.

To remove the damage layer and projections from the welding region, and to obtain clean copper surfaces various treatments are used: tumbling, chemical, and electrochemical polishing. Tumbling is carried out in horizontal position, the cavity is about half filled with ceramic chips. For chemical polishing three solutions are used containing nitric and sulfuric acid, ammonium persulfate, and sulfamic acid with hydrogen peroxide [5]. Electrochemical polishing is done in an aqueous solution containing phosphoric acid and butanol; the current density is 1.8 to 2.0 $A/dm^2$, the voltage 17 to 20 V, the temperature 14 to 17°C. The cathode is shielded with a diaphragm to avoid contamination of the copper surface with the hydrogen developed at the cathode [6].

Up to now only one coating was carried out after cleaning with sulfamic acid or by electropolishing. Some problems were experienced with rinsing and adhesion of the deposited films. More experiments have to be done to draw conclusions.

The treatment with the ammonium persulfate produces strong etching and roughening of the surface, if compared to the other treatments.

As the niobium layer can be dissolved in a solution containing fluorides without attacking the copper [4], the same cavity can be used for various coating cycles. After removing the niobium layer, a cavity is tumbled to lose the memory of the last chemical treatment, than chemically treated, and prepared for the next coating.

### 2.2 Sputter devices and sputter parameters

The study of niobium coatings on copper was started at CERN in 1980 with the development of a bias diode configuration. A magnetron sputter device, which is mechanically easier to handle and has a much higher coating rate was developed in 1985. Both systems and the experiments optimising the sputter parameters are described in [2,7,8]. Fig. 1 shows a schematic view of the systems. The sputtering parameters and the resulting niobium layer thicknesses are given in table 1.

The two coating methods result in niobium films of different aspects. As pointed out in [2] the bias diode produced films of fine crystalline structure at the equator, changing to a coarse structure at the iris. The magnetron sputtered layers present a smooth, nearly amorphous aspect. But the surface of the niobium film reproduces the structure of the copper surface in both cases. Fig. 2 gives the electron microscope pictures of a diode and of a magnetron sputtered sample, both taken from a region near the equator.

With unchanged sputter parameters the niobium film thickness is proportional to the sputter time in each system. Assuming a London penetration depth of 50 nm a layer thickness of .5 µm is sufficient to avoid losses by the penetration of the r.f.-field into the normal conducting copper substrate.

Up to now 17 niobium layers on 4 different cavities were produced with the bias diode, while 5 layers were sputtered on 3 cavities by means of the magnetron configuration.

After the deposition of the niobium layer the surfaces are inspected and rinsed with ultra pure water. If the inspection shows no film peel off and no niobium film particles are found in the rinsing water the cavity is dried in a dustfree hut (class 100) before being mounted for testing.

## 3. RESULTS AND DISCUSSION

Beside the tests related directly to the LEP application, namely the measurements of the quality factor and the accelerating field at 4.2 K, first experiments were performed to study the influence of the external magnetic field, of the cooling down velocity, and of the thermal cycling. Furthermore material parameters were investigated.

### 3.1 Q values and accelerating fields

For practical application the accelerating field ($E_{acc}$) and the quality factor (Q) are of utmost importance. Q factors and accelerating fields at 4.2 K are listed in table 2 for all niobium coated copper cavities. (The measurements of the coatings 1.1 to 3.2 are already published [8]). At low fields Q values up to $4.2 * 10^9$ are measured, considerably higher than the typical Q of $3 * 10^9$ of bulk niobium cavities [9]. Accelerating fields of 8 MV/m are reached reproducibly; the maximum accelerating field was about 11 MV/m. All these values are comparable to those achieved with the niobium cavities. The fields were power limited due to a strong reduction of the Q value except in one case. In this case the field was limited by a quench. Temperature mapping revealed a needle like, bent copper particle at the quench location on the equator. The power limitation is due to the type N connectors which are used in the experiment: a safe operation is possible up to about 200 W input power. At the LEP design field of 5 MV/m the obtained values of Q reproducibly lie between $1.5 * 10^9$ and $1.9 * 10^9$. At the highest accelerating fields the Q degradation is due to non-resonant electron loading. At lower fields three types of Q(E) degradation were observed, which will be discussed in the following.

### 3.2 Dependence of Q on the accelerating field

Fig. 3(a) shows the Q(E) of a cavity with blisters. The copper surface is completely covered with niobium, but in small areas the niobium film is in poor thermal contact with the cavity wall, due to bad adhesion. At low fields - or low incident powers - the heat transfer is sufficient to keep this defect well below the critical temperature. At some definite power, depending on the location in the cavity and on the geometry of the defect, a thermal runaway occurs and the area becomes normal conducting, resulting in a sudden reduction of Q (Q switch). Bad adhesion is known to be due to dust, impurities in or on the surface, purity of the chemicals, etc. Fig. 4 for example shows the electron microscope pictures of an inox-titanium particle (a) and of the impression of a dust particle (b). Both impurities were sitting on the copper side of small niobium pieces. They were peeled off with adhesive tape from the surface of a cavity. The temperature maps of a cavity with two blisters are shown in fig. 5. Fig. 5(a) shows the losses before the Q switches. The additional losses produced in the blisters are indicated in figs 5(b) and 5(c).

Fig. 3(b) shows the Q(E) curve of a cavity with an uncomplete niobium layer, the Q(4.2 K) is already $1.5 * 10^9$ at the lowest measurable fields: the temperature map shows a point of enhanced losses. The inspection showed at this location an uncovered copper area [4]. The strong decrease at low fields may indicate small regions which have reduced superconducting properties or are even normal conducting. Normal conducting regions in the submicron range can initially be hidden by the proximity effect and become normal conducting with increasing field [10].

Fig. 3(c) gives the third type of Q(E) dependence. Q decreases exponentially with the field and can be parametrised as

$$Q(4.2\ K, E) = Q(4.2\ K, 0) * \exp(-\alpha * E)$$

At 4.2 K this equation holds for a large region of the Q(E) plots, with $\alpha$ varying between .07 and 2. In the literature the field dependent Q degradation is interpreted as an effect of the surface roughness [11,12]. It is assumed that at tiny peaks, at etched grain boundaries for example [12], the critical magnetic field of the superconductor is exceeded and with increasing fields more and more points are becoming normal conducting, reducing the Q quasicontinuously. For the case of corners the enhancement factor of the magnetic field is calculated to grow proportionally to $r^{-1/3}$, where r is the corner radius [13].

3.3 <u>Temperature dependence of Q(E)</u>

Fig. 6 shows the Q(E,T) measurements of the first magnetron sputtered cavity. This cavity had a residual Q of about $6 * 10^{10}$, the highest Q reached with a 500 MHz cavity at CERN. The measurements at 3.1 K and 2.4 K are parametrised by the equation:

$$Q(T,E) = \left[ \frac{\exp(\alpha * E * (H_c(4.2\ K)/H_c(T))^2) - 1}{Q(4.2\ K, 0)} + \frac{1}{Q(T, 0)} \right]^{-1}$$

The first term on the right hand side of this equation determines the temperature dependence of the losses which are induced by the accelerating field. The influence of the temperature is correlated only to the temperature dependence of the superconducting critical field $H_c(T)$

$$H_c(T) = H_c(0) * (1 - (T/T_c)^2) \quad .$$

The second term is the surface resistance at the bath temperature at very low fields. Field enhancement due to the surface roughness can explain the Q degradation and the fitted temperature dependence, supporting the model given above.

### 3.4 Q degradation and surface roughness

To study the correlation between the Q degradation and the surface roughness, the chemical treatment of the cavities was applied to samples made from the same OFHC copper. The tumbling which is difficult to applicate on samples was replaced by mechanical polishing. The surfaces of the samples were inspected by means of a scanning electron microscope, and their roughness was measured.

In fig. 7 the aspects and roughness measurements after a sulfonitric and a repeated ammonium persulfate treatment are given as an example. The pictures show a smooth surface after the sulfonitric (b), and a heavily etched copper surface after the persulfate treatment (a). There is no clear correlation between the measured maximum and/or average roughness ($R_T$ and $R_A$) and the slope of the Q(E) curve. But the number of peaks for a given length is strongly related to the values of $\alpha$, as shown in fig. 8. We define as "peak" any point which has a height larger than twice the width in the measured roughness plot.

Extrapolation to very smooth surfaces shows that values of $\alpha$ as small as 0.05 might be reached, which are comparable to those measured on 500 MHz niobium sheet cavities.

### 3.5 The influence of external magnetic fields, thermal cycling, and cooling

It is well known (f.e. [11]) and also observed at CERN on 500 MHz niobium cavities [9] that external magnetic fields increase the residual resistance of superconducting resonators. To shield the cavity from the earth magnetic field the experimental cryostat is surrounded by compensation coils which reduce the ambient field to 20 mG. Furthermore experiments at the ambient field and at two times the ambient field can be done. Measurements at these three fields were carried out on a niobium coated copper cavity and a niobium sheet cavity, both showing about the same Q values at low fields. In fig. 9 the inverse of the residual Q is plotted against the external magnetic field. The residual Q of the coated copper cavity is hardly influenced by the external fields, while the residual Q of the niobium cavity is reduced by more than a factor of ten at the maximum applied field. The feature and the origin of this effect are at present under study.

Thermal cycling was found to lead to a peel off of the niobium film sputtered on samples after several cooldown cycles by immersion in liquid nitrogen. But after repeating five times cooldown from room temperature to 4.2 K no influence was seen on the initial Q factor nor on Q(E) measured on a niobium coated copper cavity.

Fast cooling is known to increase the surface resistance of cavities made from layered composite materials [11,14]. Frozen in flux, induced by thermoelectric currents is assumed to produce the additional losses. Cooling down a coated cavity within half an hour or half a day had no influence on the Q values at 4.2 K.

### 3.6 Material parameters

To study material parameters of niobium coatings the temperature dependence of the Q value was measured for different films and compared to that obtained from niobium sheet cavities. As an example Q(T) for two different layers is given in fig. 10. The Q value is related to the surface resistance $R_s$ via

$Q = G/R_s$ where G is the geometry factor.

Following the BCS theory the superconducting surface resistance is described by the equation:

$$R_s(T) = (A/T) * \exp -(\Delta * T_c/T) + R_{res} \text{ for } < T_c/2$$

$$= R_s^{BCS}(T) + R_{res}$$

with:

| | |
|---|---|
| $R_s^{BCS}(T)$ = | temperature dependent theoretical surface resistance. |
| $R_{res}$ = | residual, temperature independent surface resistance. |
| A = | constant containing the free mean path l, the superconducting penetration depth $\lambda$. |
| $2\Delta$ = | the superconducting energy gap. |
| $T_c$ = | the superconducting critical temperature. |

With a $T_c$ of (9.25 ∓ 15)K measured on samples and on coated cavities we calculated $R_s^{BCS}$ (4.2 K), $R_{res}$, $\Delta$, and A via the fit program MINUIT [15]. The calculated values are given in table 3. The variation of $R_s^{BCS}$ (4.2 K) with RRR is shown in fig. 11. This figure shows a good agreement between our measurements and the RRR - or mean free path - dependence of the BCS resistance calculated by Halbritter [16] and by Martinez and Padamsee [17]. Moreover we find a good agreement even in the absolute BCS surface resistance if we replace the energy gap given in [17] by our measured value.

## 4. CONCLUSION

At CERN two sputtering configurations were developed which are able to produce high quality niobium films on 500 MHz single cell cavities, a bias diode and a magnetron. With both systems niobium coated copper cavities were obtained which reproducibly reach Q factors of $(3.5 \mp .5) * 10^9$ at 4.2 K and at low fields. Q values at the LEP machine design field of 5 MV/m ranged up to $1.9 * 10^9$. These performances are comparable to those measured on niobium sheet cavities.

Only once the accelerating field was limited by quenching, provoked by a defect of the copper surface at the equator. Usually the field is power limited between 8 and 9 MV/m, but in one case a field of 11 MV/m was reached.

Radiofrequency measurements combined to surface studies demonstrated the influence of the roughness of the copper surface on the high field performances of the cavities. To reach high Q values at high accelerating fields already very smooth copper surfaces are required.

The studies of the superconducting material parameters show that the Q values of niobium coated copper cavities can be superior to those of very pure niobium cavities.

In the next step we have to translate our knowledge to the fabrication of a four cell, 350 MHz LEP type structure (fig. 12). This cavity is already built. The elements for a bias diode configuration are ready. First sputter experiments are running to study the performances of the niobium film on samples. We hope that with an adapted chemical treatment and under clean preparation conditions the 4-cell niobium coated copper cavities will show performances comparable to those of the niobium sheet cavities.

Acknowledgements

J. Genest has designed the cathodes of the magnetron and of the diode configuration. The electron microscope photographs were taken by J. Adam. Surface roughness was measured by R. Rossari, critical temperatures by M. Blin.

All power supplies were designed and purchased by R. Genand and A. Delezée. Chemical treatments were suggested and carried out by J.P. Birabeau, A. Boulmier, J. Guerin and R. Kopp.

The authors are indebted to Ph. Bernard and H. Lengeler for continuous encouragement and stimulating discussions and to all technicians of the RF group who prepared and helped to perform the r.f.-tests.

REFERENCES

[1] G. Arnolds-Mayer et al., Vancouver Accelerator Conference 1985.

[2] C. Benvenuti et al., J. Appl. Phys. 45 (1984) 583.

[3] H. Padamsee, IEEE Trans. Magn. MAG-19 (1983) 1322.

[4] N. Circelli, CERN/EF/RF 85-5 (1985).

[5] J. Adams et al. (in preparation).

[6] D. Bloess and L. Ponto (in preparation).

[7] C. Benvenuti et al., IEEE Trans. Magn. MAG-21 (1985) 153.

[8] N. Hilleret et al. (in preparation).

[9] P. Bernard et al., Nucl. Inst. Meth. 206 (1983) 47.

[10] W. Schwarz and J. Halbritter, J. Appl. Phys. 48 (1977) 4618.

[11] J.M. Pierce, J. Appl. Phys. 44 (1973) 1342.

[12] Y. Uzel, K. Schnitzke and N. Krause, Appl. Phys. A30 (1983) 185.

[13] P. Kneisel et al., IEEE Trans. Magn. MAG-21 (1985) 1000.

[14] M. Peiniger and H. Piel, Vancouver Accelerator Conference 1985.

[15] F. James and M. Roos, CERN Program Library D506, D516.

[16] J. Halbriter, Zeit. für Physik C238 (1970) 466.

[17] E. Martinez and H. Padamsee, Rep. SR4 841201-EX Cornell University, 1984.

# TABLE 1

Sputter parameters and niobium layer thicknesses
for the bias diode and magnetron configuration

| Sputtering configuration | Bias diode | Magnetron |
|---|---|---|
| Sputter voltage | 1400 V | 700 V |
| Bias voltage | 80 V | - |
| Magnetic field | - | 100 G |
| Argon pressure | $5 * 10^{-2}$ Torr | $2 * 10^{-4}$ Torr |
| Sputter time | 24 h | 50 min. |
| Layer thickness | 1.2 µm (equator)<br>4.6 µm (iris) | 1.2 µm ± 20% |

TABLE 2

Q-values and accelerating fields at 4.2 K

Legenda: Cav.: number of cavity and layer;

Preparation of the copper surface (Cu): T: 7 days tumbling, N: nitric acid;

P: ammonium persulfate; E: electrochemical polishing; S: sulfamic acid;

Preparation of the niobium layer: Dn, Mn: coated by means of the bias diode (D), or magnetron (M) configuration during n hours;

Film peel off: large areas of the film peeled off, no measurement possible.

| Cav. | Preparation Cu | Preparation Film | Q ($*10^9$) .05 MV/m | Q ($*10^9$) 5.0 MV/m | $E_{max}$ MV/m | Remarks/relevant defects |
|---|---|---|---|---|---|---|
| 1.1 | T, N | D23 | 1.0 | - | .9 | Q switch |
| 2.1 | T, N | D21 | - | - | - | Film peel off |
| 2.2 | T, N | D22 | 2.5 | 1.0 | 8.6 | |
| 2.3 | | D8 | 1.5 | - | 2.4 | Q switch |
| 2.4 | N | D23 | 1.7 | .9 | 7.9 | |
| 2.5 | P | D24 | 2.5 | .8 | 7.1 | Q switch |
| 3.1 | T, D | D5.5 | .02 | - | .8 | Film peel off |
| 3.2 | P | D24 | .01 | - | .14 | Poor performance not understood |
| 3.3 | N | D24 | 4.0 | 1.2 | 10.8 | Q switch |
| 3.3 | Baked at 120°C | | | | | Film peel off |
| 3.4 | P | D12 | 2.0 | - | 4.5 | |
| 3.5 | P | D32 | 3.5 | - | 2.5 | Q switch |
| 3.6 | T, N, P | D24 | 3.5 | 1.9 | 9.1 | |
| 3.7 | N, P | D12 | 3.5 | 1.3 | 8.7 | |
| 3.8 | N, P | M.8 | 4.2 | 1.6 | 8.1 | |
| 3.9 | T, N, P | D12 | 2.5 | 1.2 | 8.6 | |
| 3.10 | T, N | D12 | - | - | - | Film peel off, no fresh acid |
| 3.11 | T, N | D12 | 3.1 | 1.7 | 8.3 | |
| 3.12 | T, N | M.8 | - | - | - | Film peel off, heavily oxidised |
| 4.1 | T, N, P | D24 | 2.9 | 1.0 | 7.6 | Quenching |
| 4.2 | T, N | M.8 | > 1.0 | - | - | Leak at 4.2 K |
| 4.3 | T, E | M.8 | 3.5 | - | 1.9 | Q switch |
| 5.1 | T, S | M.8 | 4.0 | 1.5 | 8.1 | Q switch |

## TABLE 3

Material parameters for niobium

Legenda: H2, H3, C3: 500 MHz cavities made from sheet material, others see table 2.
RRR: residual resistivity ratio; all values measured;
λ: thermal conductivity: H2, H3, C3 measured, other calculated;
Δ: superconducting energy gap, error < 0.1%;
A: normalisation constant, error 5 to 10%;
$R_{res}$: residual resistance, error 5 to 10%;
$R_s^{BCS}$: theoretical surface resistance, error 5 to 10%.

| | H2 | H3 | C3 | 3.6 | 3.7 | 3.8 |
|---|---|---|---|---|---|---|
| RRR | 100 ∓ 10 | 100 ∓ 10 | 35 ∓ 5 | 9-14 | 9-14 | 3-9 |
| λ(W/K m)<br>Nb at 4.2 K<br>Cu at 4.2 K | <br>25-30 | <br>25-30 | <br>7.5-10 | <br>2-3.5<br>460 | <br>2-3.5<br>460 | <br>1-2.2<br>460 |
| $\Delta(k_B T_c)$ | 1.98 | 1.98 | 1.98 | 1.98 | 1.98 | 1.98 |
| A (*$10^{-5}$) (ΩK) | 3.3 | 2.7 | 2.4 | 1.9 | 2.0 | 2.0 |
| $R_{res}$ (nΩ) | 76 | 11 | 17 | 15 | 13 | 4 |
| $R_s^{BCS}$ (4.2 K) (nΩ) | 100 | 81 | 73 | 59 | 61 | 59 |

## FIGURE CAPTIONS

Fig. 1 Schematic view of the sputtering configurations: (a) bias diode; (b) magnetron.

Fig. 2 Surfaces of niobium films on samples. (a) Diode deposited; (b) magnetron deposited (white bar ≙ 1 µm).

Fig. 3 Types of Q(E) dependence.

Fig. 4 Copper side from niobium particles peeled off from a niobium coated copper cavity. (a) Impurity of inox-titanium; (b) impression of dust particle (white bar ≙ 10 µm).

Fig. 5 Temperature maps of a cavity with blisters.

Fig. 6 Measured and calculated Q(E) dependence.

Fig. 7 Surface structures and roughness measurements from copper samples (white bar ≙ 1 µm).

Fig. 8 Slope of Q(E) as function of the surface roughness.
(N: number of peaks from surface measurement roughness).

Fig. 9 Influence of external magnetic fields on the residual resistance.

Fig. 10 Temperature dependence of Q for two niobium coated copper cavities ($T_c$ = 9.25 K).

Fig. 11 Normalized BCS surface resistance at 4.2 K for niobium of different residual resistivity ratio (RRR):

- - - - from J. Halbritter [16];

______ from E. Martinez, H. Padamsee [17];

RRR 25 from P. Bernard et al. [9].

Fig. 12 4-cell 350 MHz accelerator structure.

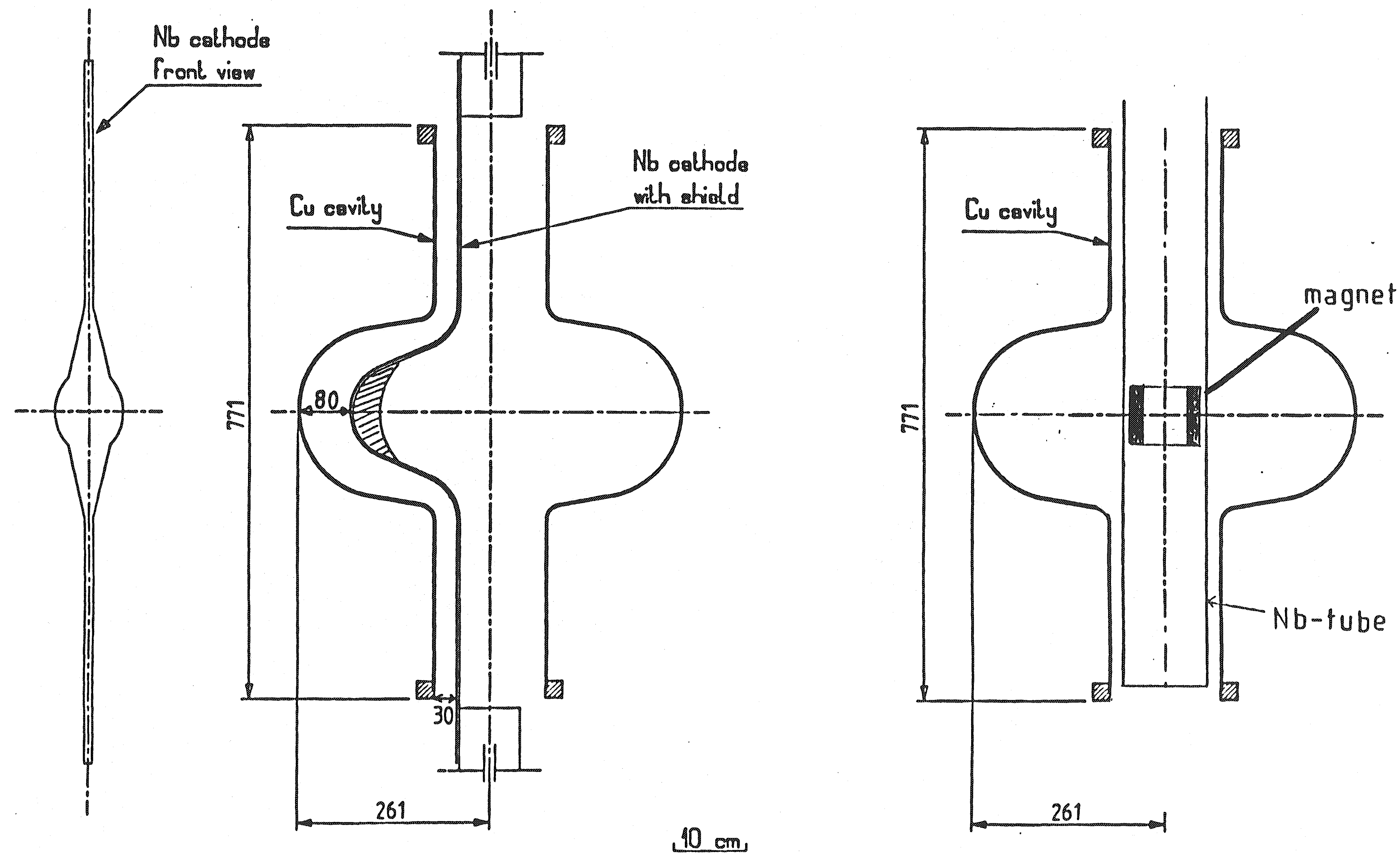
Nb cathode
front view
Cu cavity
Nb cathode
with shield
80
771
30
261
10 cm
Cu cavity
magnet
771
Nb-tube
261

(a) (b)

Fig. 1

(a)

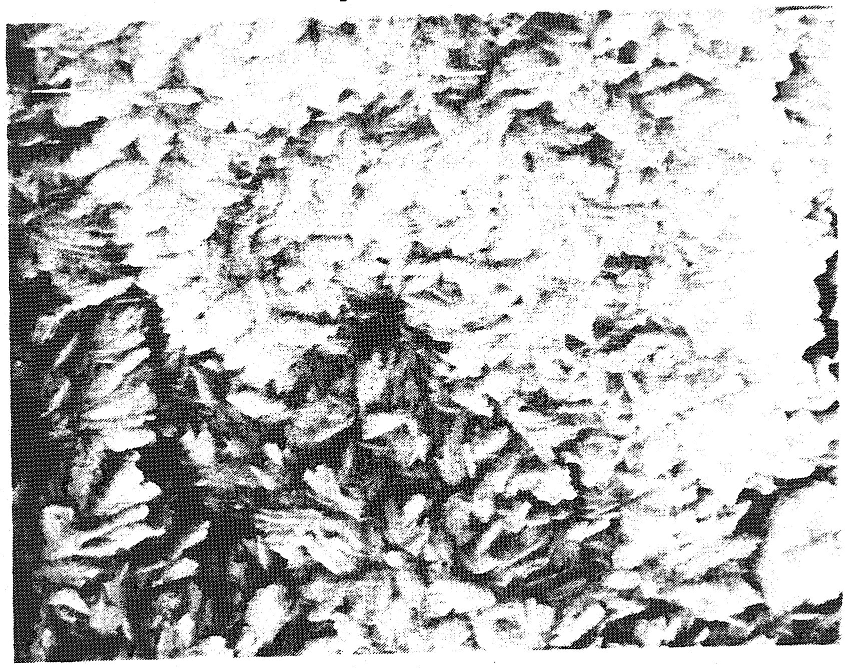

(b)

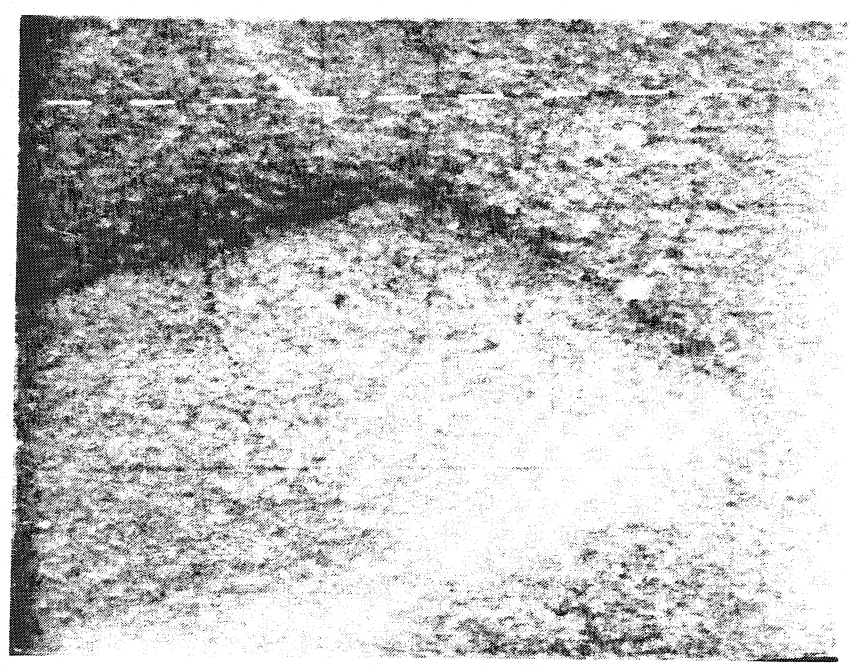

Fig. 2

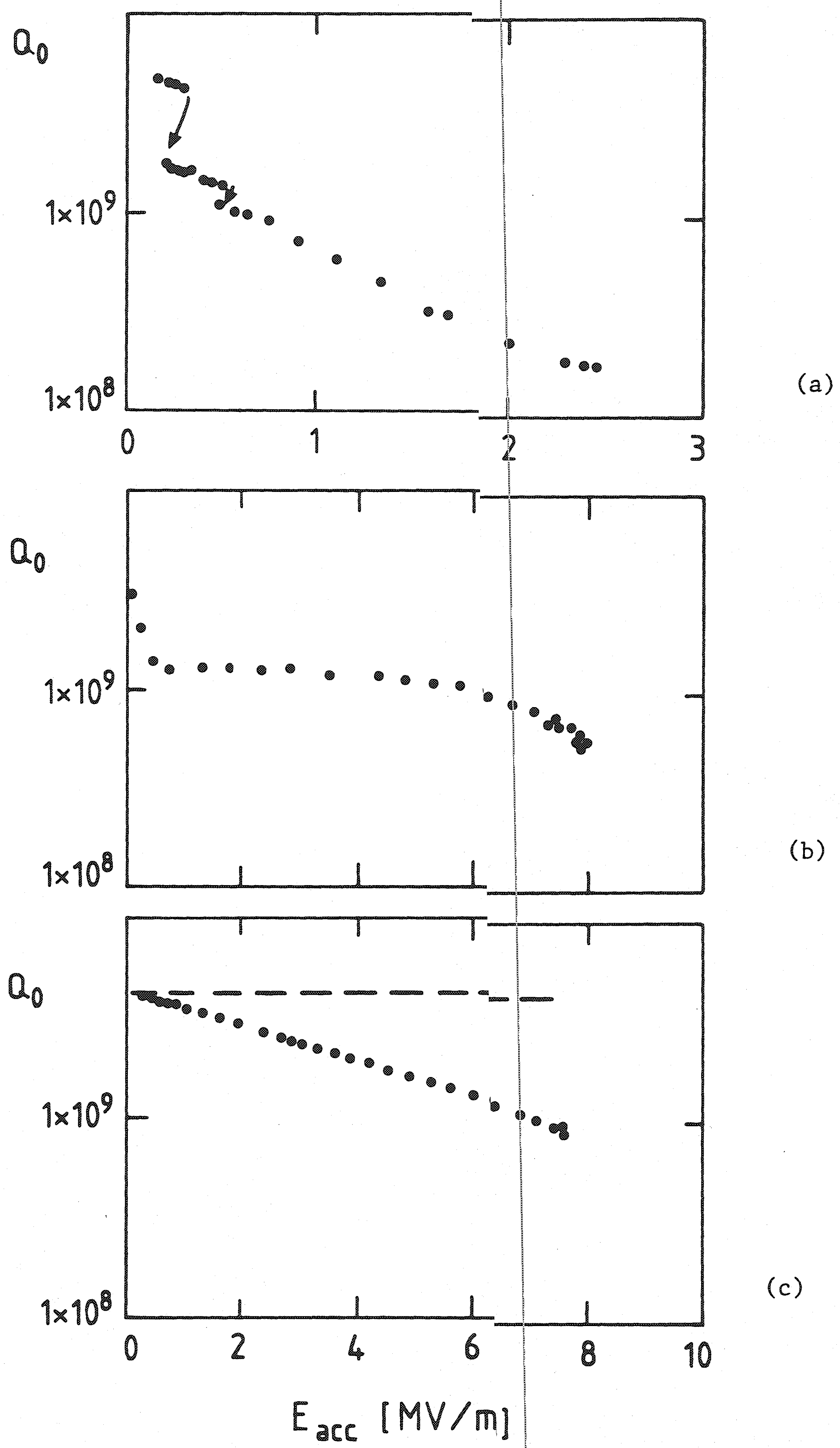
Q0
1×10^9
1×10^8
0
1
2
3
(a)
Q0
1×10^9
1×10^8
(b)
Q0
1×10^9
1×10^8
0
2
4
6
8
10
(c)
E acc [MV/m]

Fig. 3

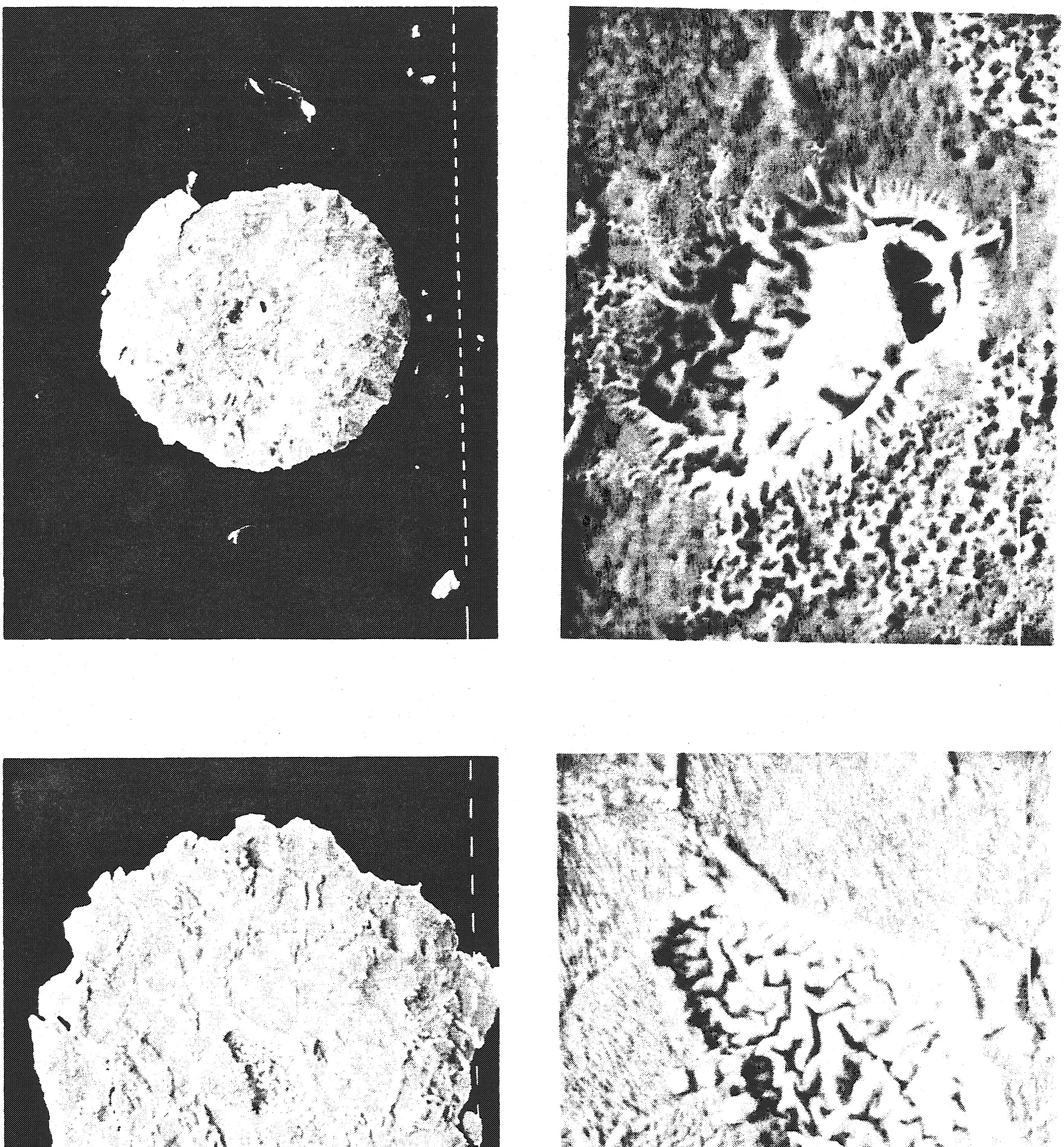

(a)

(b)

Fig. 4

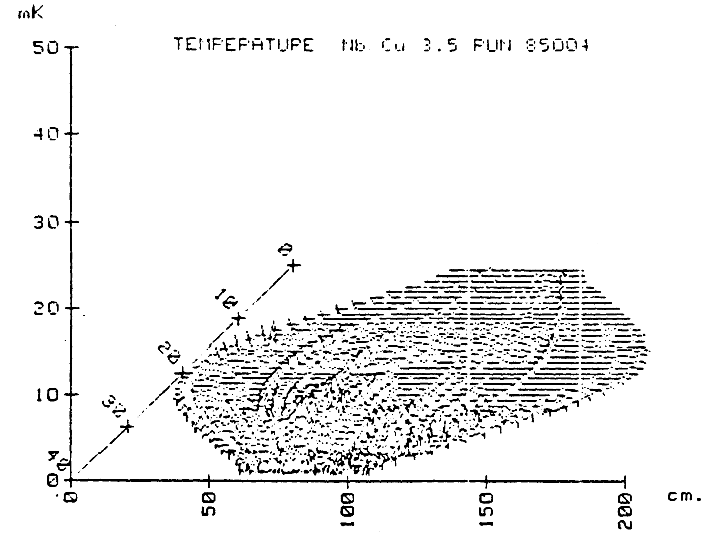


$T_{bath}$ = 2.7 K

$E_{acc}$ = 0.33 MV/m

$Q_0 = 4.5 \cdot 10^9$

(a)

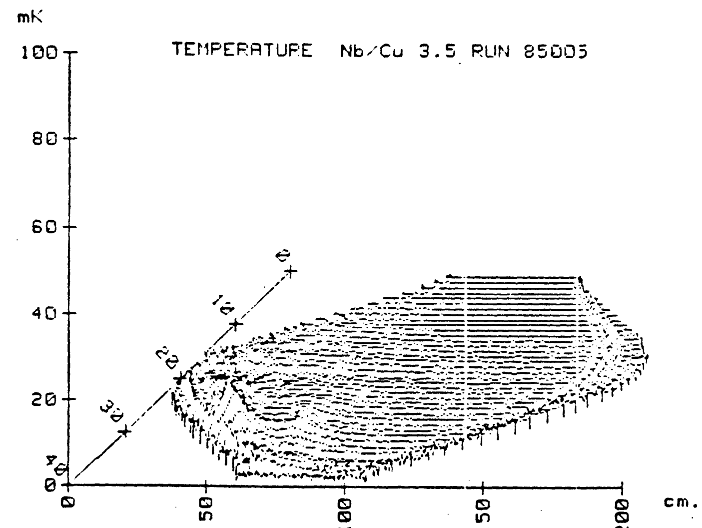


$T_{bath}$ = 2.2 K

$E_{acc}$ = 0.35 MV/m

$Q_0 = 1.7 \cdot 10^9$

(b)

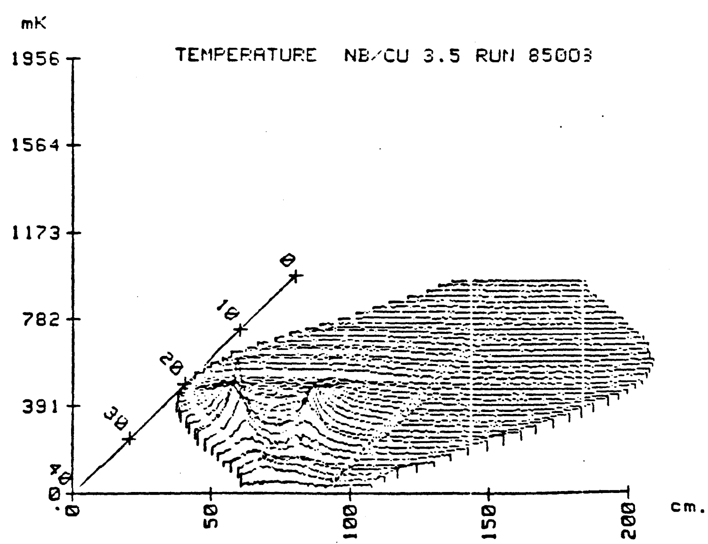


$T_{bath}$ = 2.75 K

$E_{acc}$ = 1.18 MV/m

$Q_0 = 0.5 \times 10^9$

(c)

Fig. 5

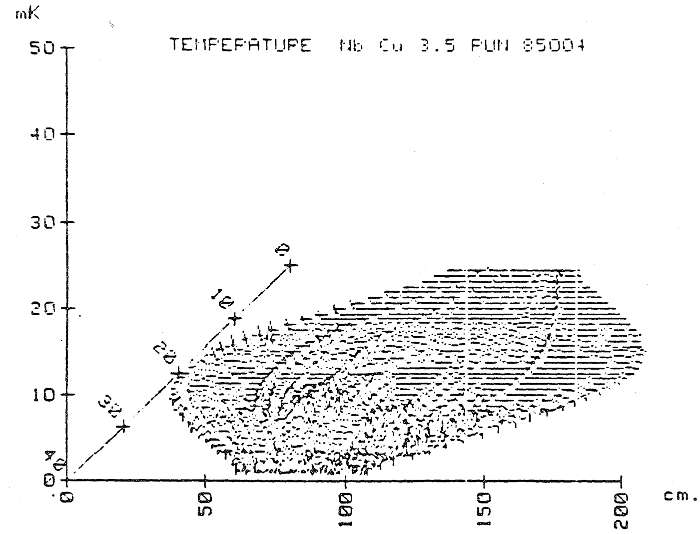


$T_{bath}$ = 2.7 K

$E_{acc}$ = 0.33 MV/m

$Q_0$ = 4.5 . $10^9$

(a)

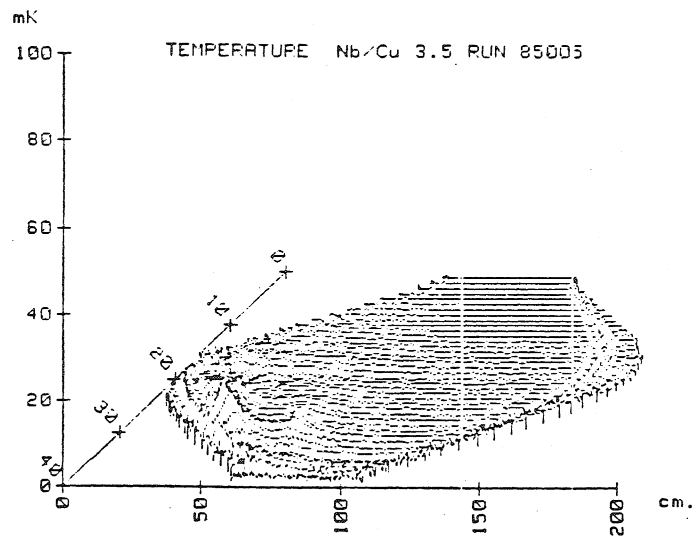


$T_{bath}$ = 2.2 K

$E_{acc}$ = 0.35 MV/m

$Q_0$ = 1.7 . $10^9$

(b)

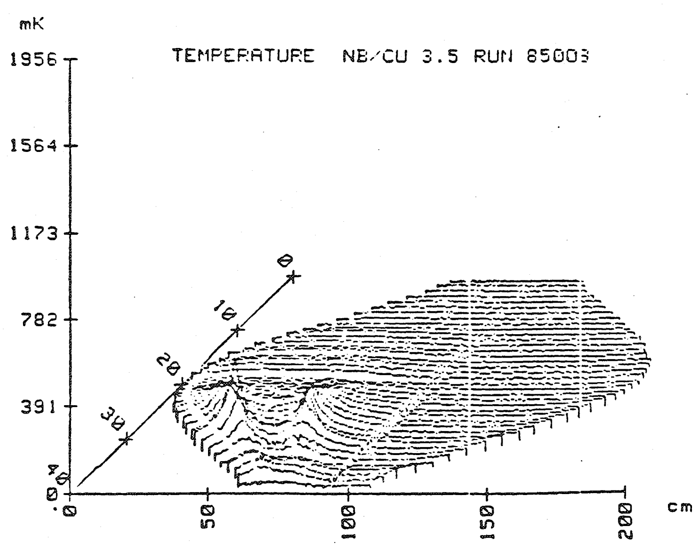


$T_{bath}$ = 2.75 K

$E_{acc}$ = 1.18 MV/m

$Q_0$ = 0.5 x $10^9$

(c)

Fig. 5

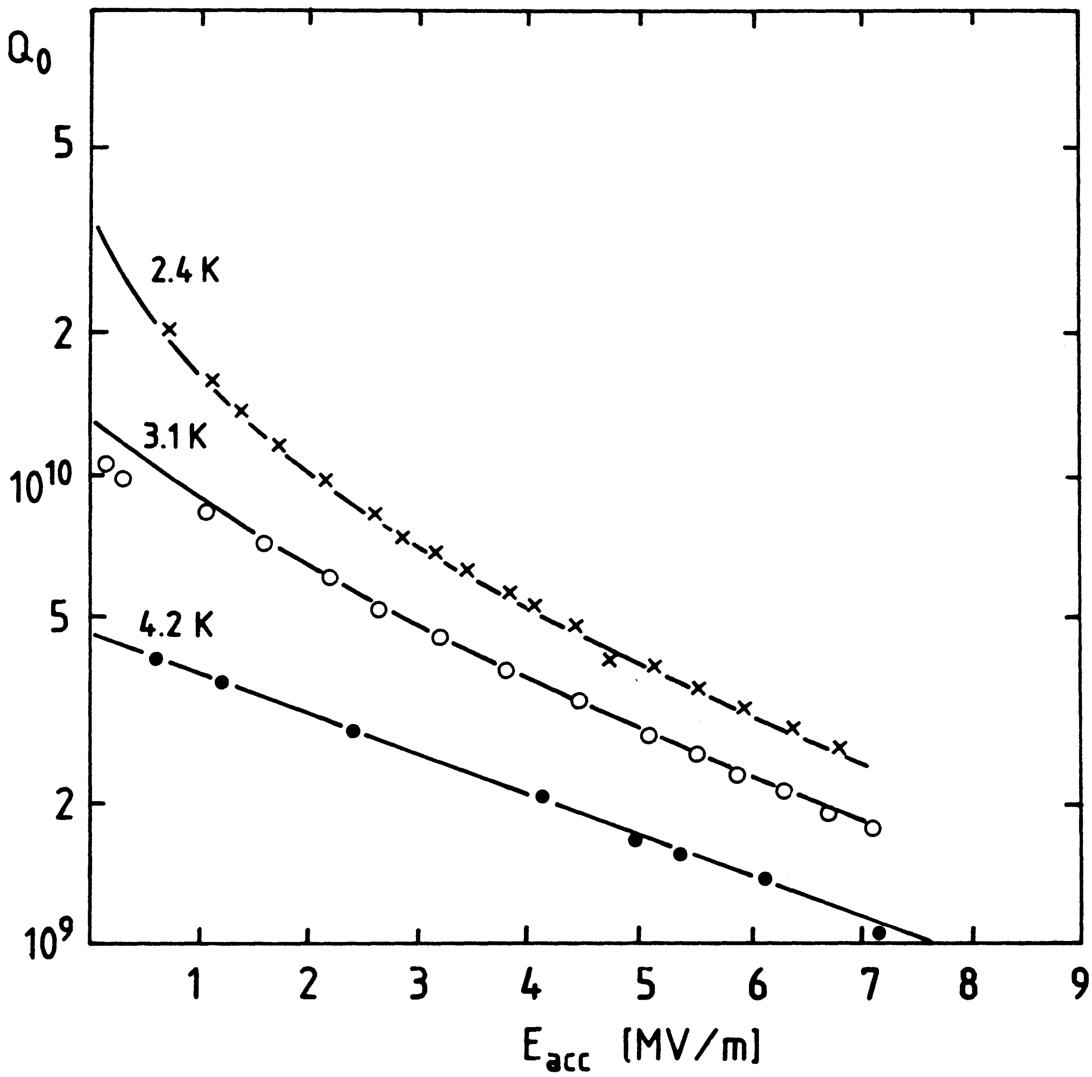


Fig. 6

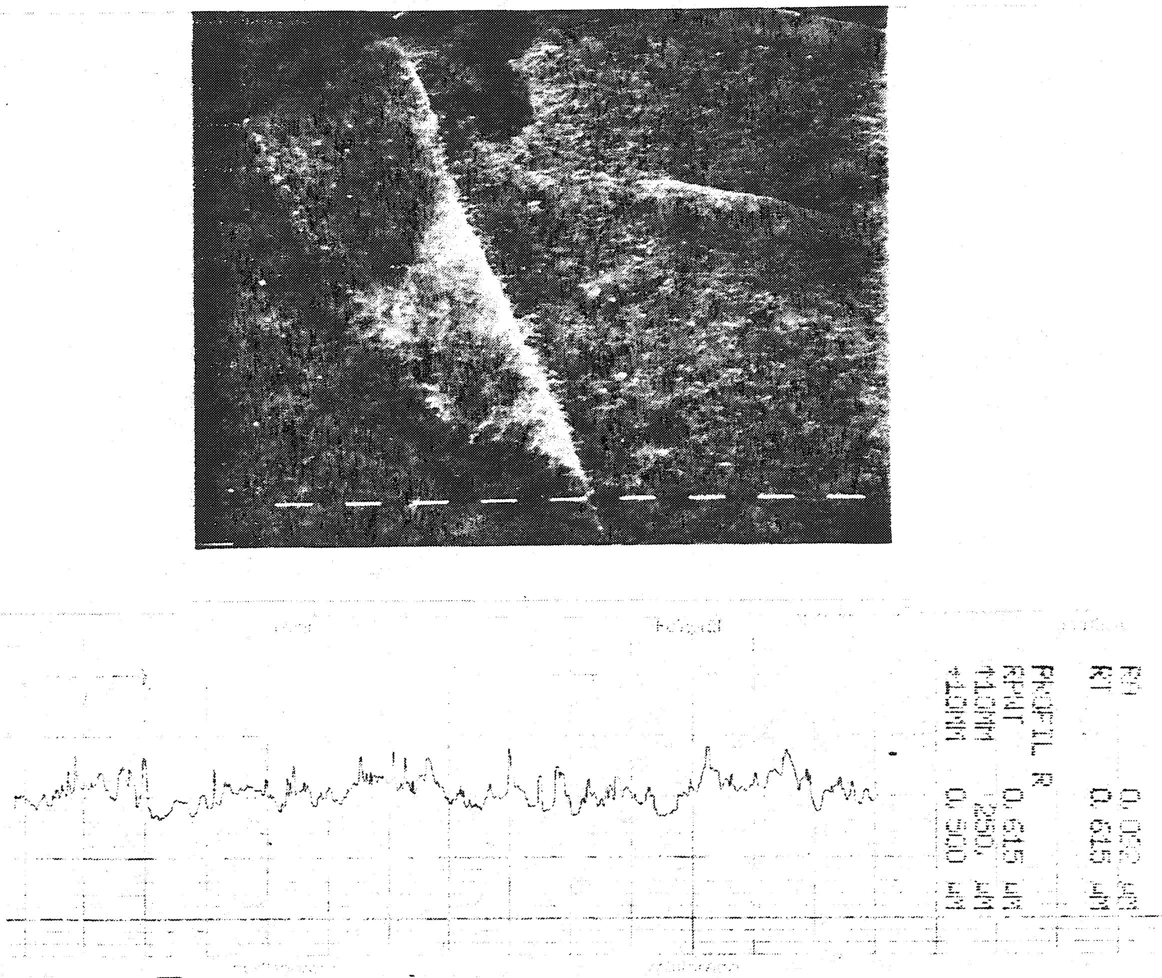
RA 0.062 µm
RT 0.615 µm
PROFIL R 0.615 µm
RPWT 250. µm
0.500 µm

(a)

Fig. 7

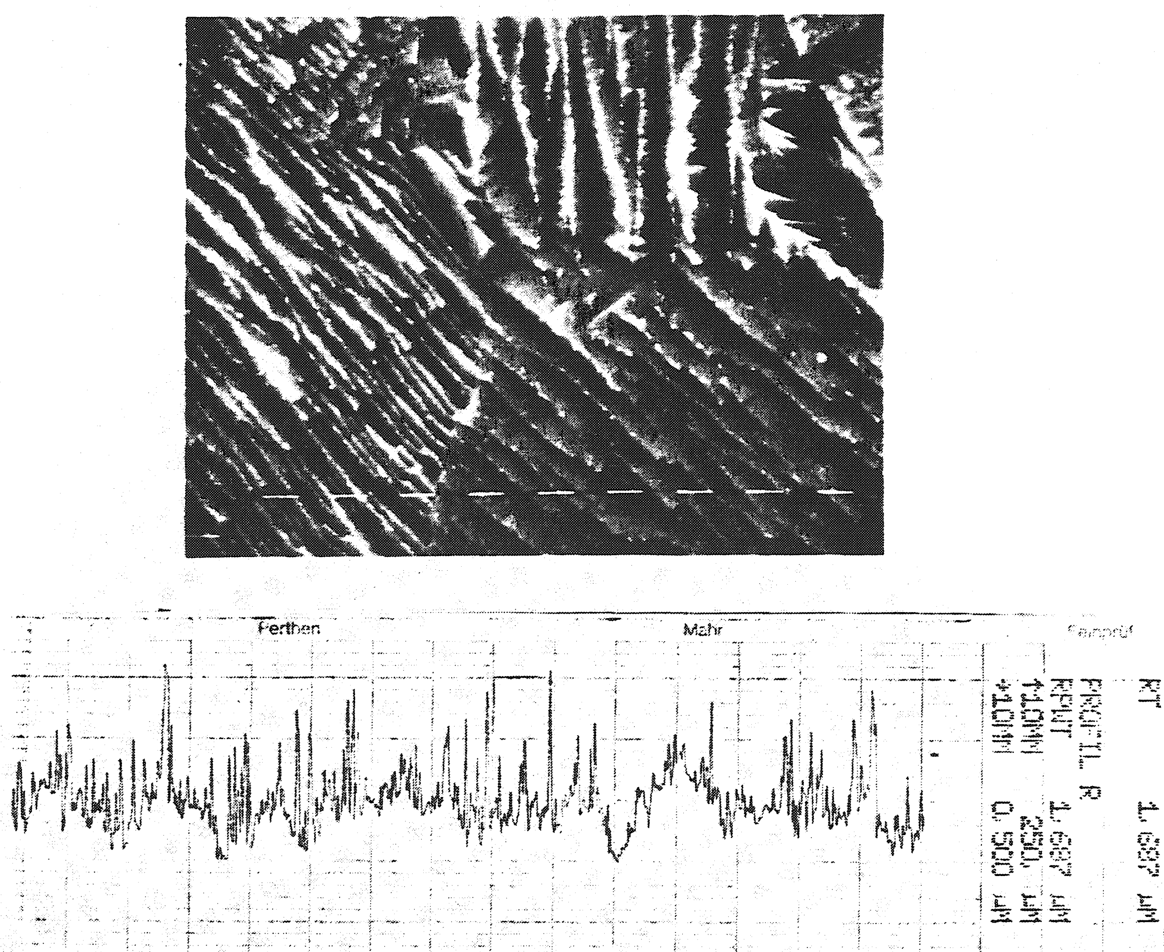
Perthen
Mahr
RA 0.152 µm
RT 1.687 µm
PROFIL R 1.687 µm
RPWT 250. µm
0.500 µm

(b)

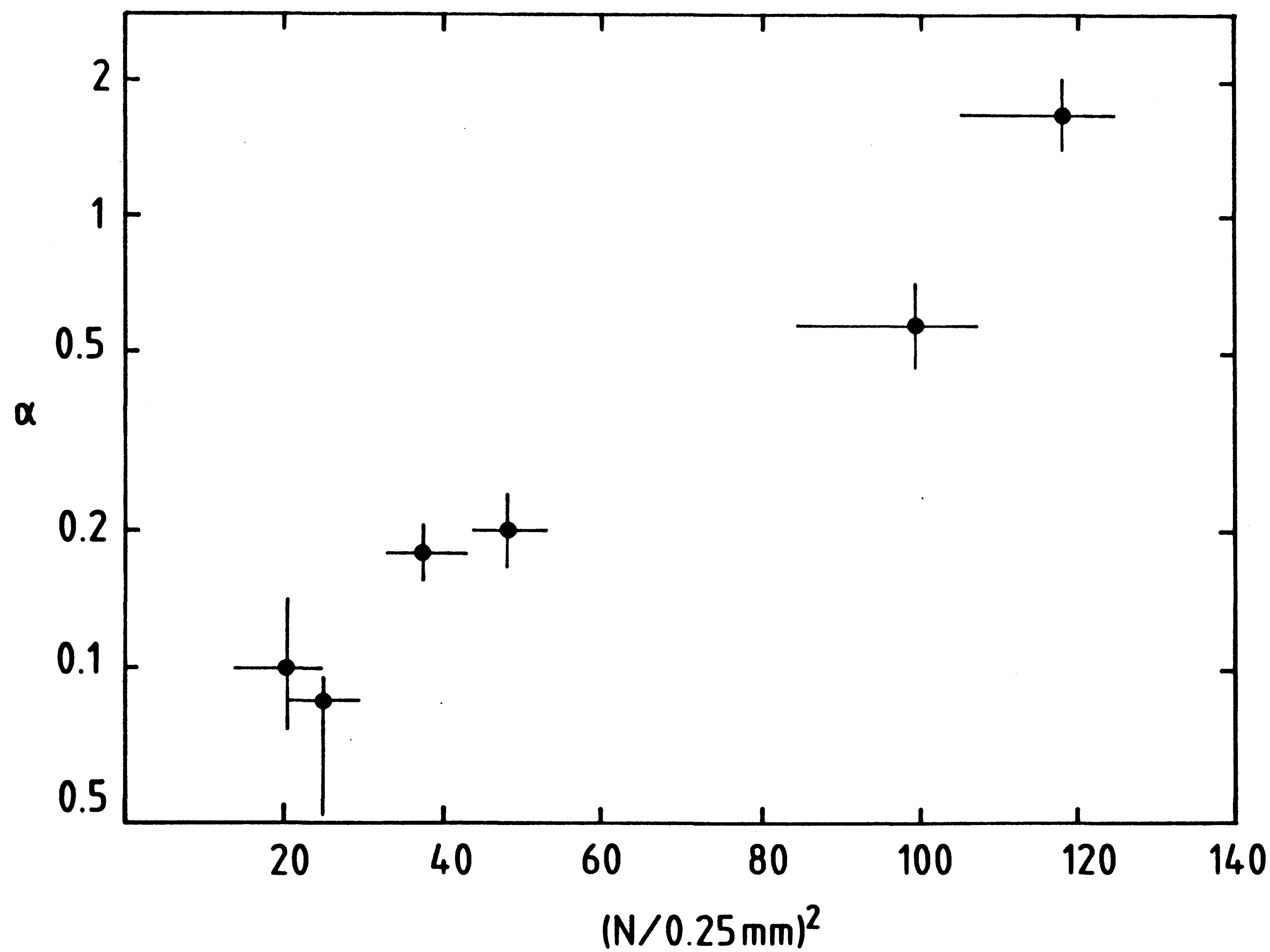


Fig. 8

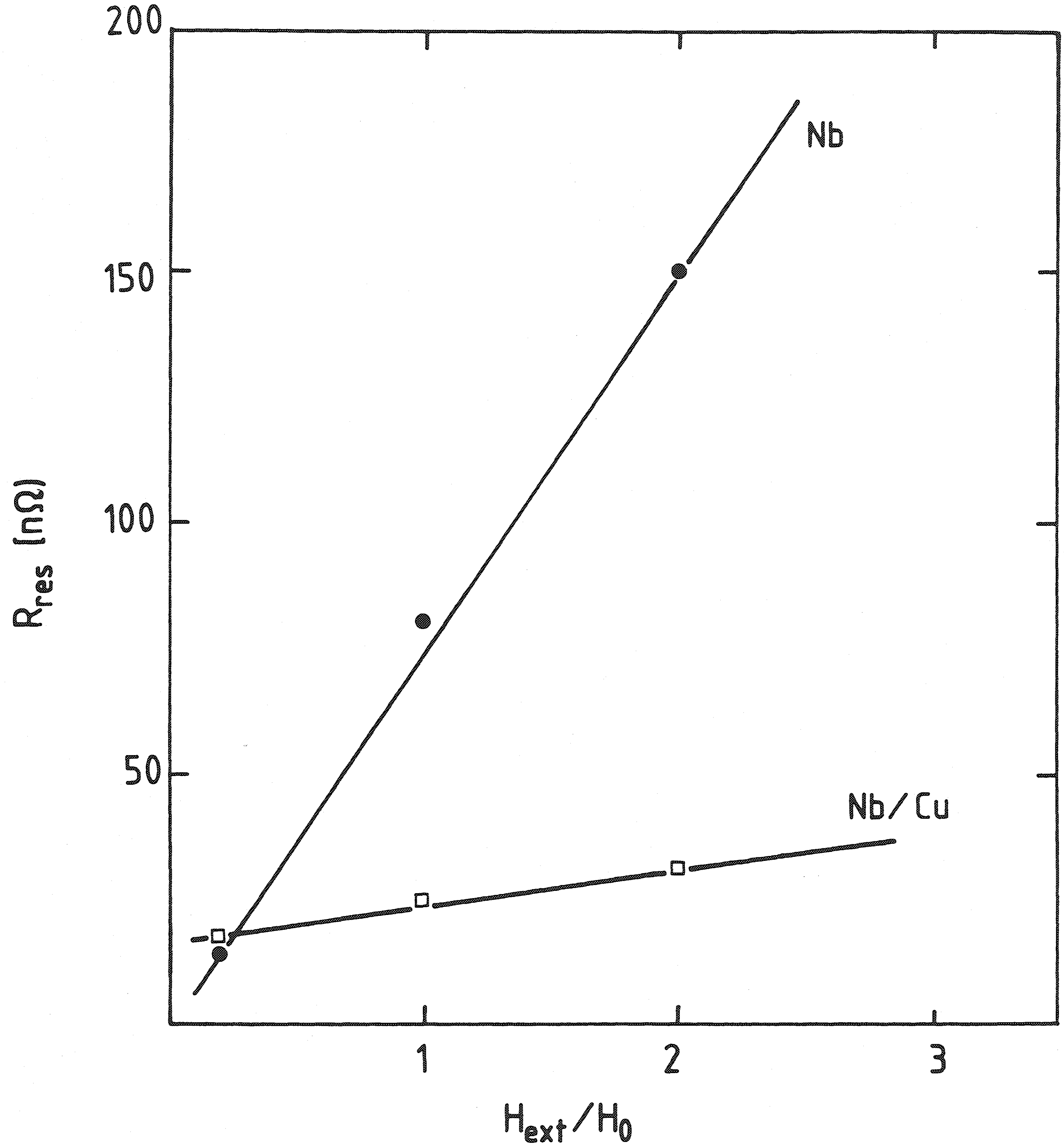


Fig. 9

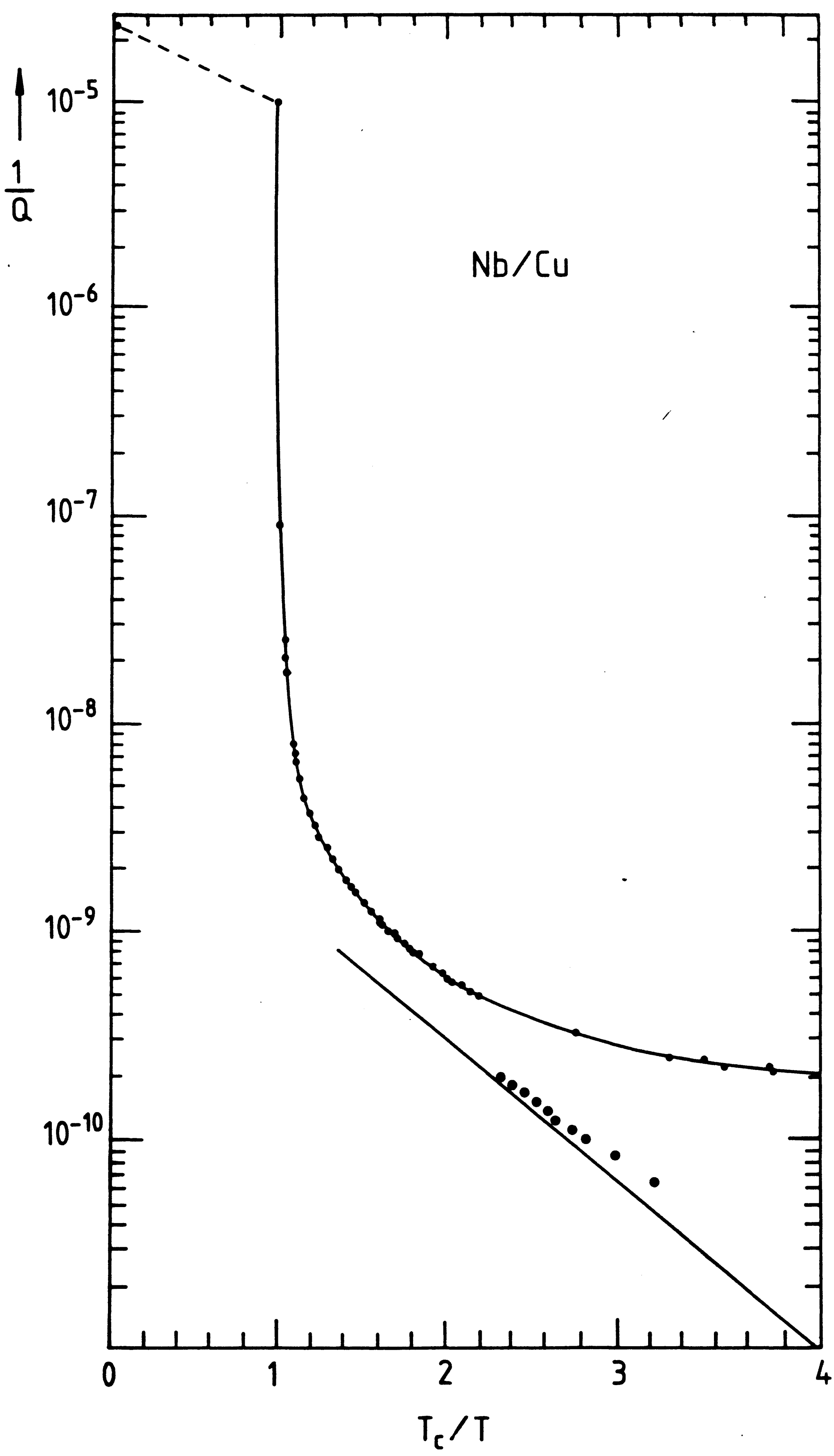


Fig. 10

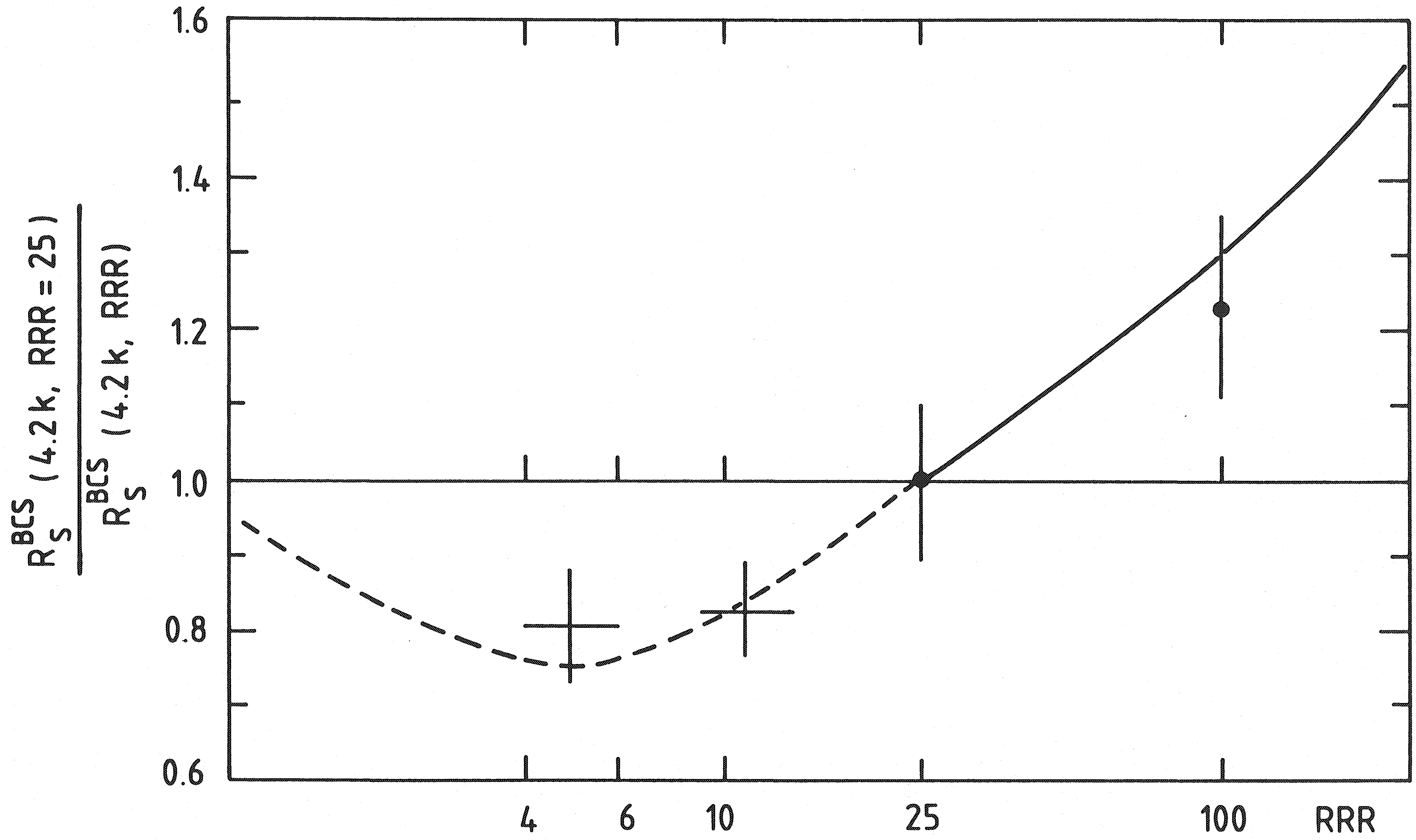

$\frac{R_S^{BCS}(4.2k, RRR = 25)}{R_S^{BCS}(4.2k, RRR)}$
1.6
1.4
1.2
1.0
0.8
0.6
4
6
10
25
100
RRR


Fig. 11

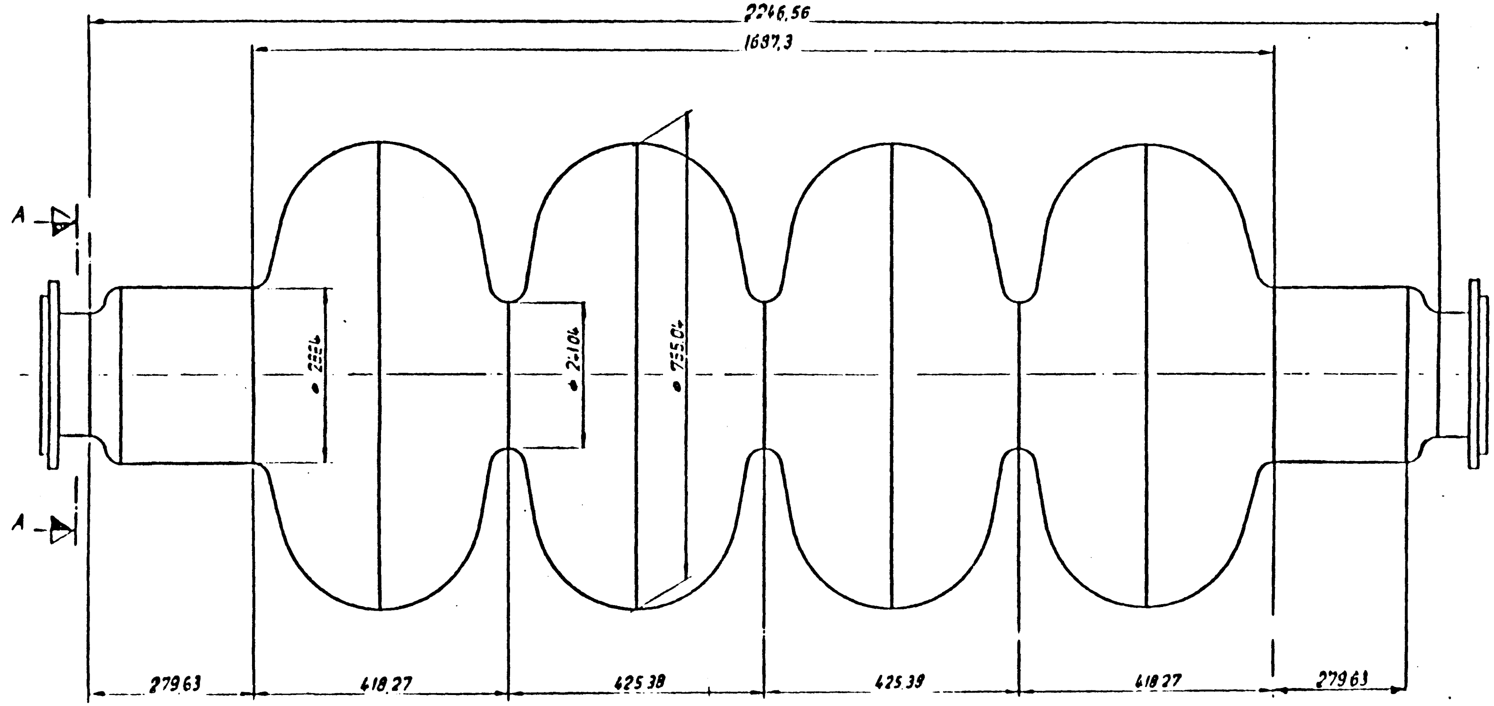

2246,56
1687,3
A
A
⌀ 225,6
⌀ 210,6
⌀ 755,04
279.63
418.27
425.38
425.39
418.27
279.63


Fig. 12